

# One at a Time: Intramolecular Electron-Transfer Kinetics in Small Laccase Observed during Turnover

Ankur Gupta, Thijs J. Aartsma, and Gerard W. Canters\*

Leiden Institute of Physics, Leiden University, Leiden, The Netherlands

**S** Supporting Information

**ABSTRACT:** Single-molecule enzymology provides an unprecedented level of detail about aspects of enzyme mechanisms which have been very difficult to probe in bulk. One such aspect is intramolecular electron transfer (ET), which is a recurring theme in the research on oxidoreductases containing multiple redox-active sites. We measure the intramolecular ET rates between the copper centers of the small laccase from *Streptomyces coelicolor* at room temperature and pH 7.4, one molecule at a time, during turnover. The forward and backward rates across many molecules follow a log-normal distribution with means of 460 and 85 s<sup>-1</sup>, respectively, corresponding to activation energies of 347 and 390 meV for the forward and backward rates. The driving force and the reorganization energy amount to 0.043 and 1.5 eV, respectively. The spread in rates corresponds to a spread of ~30 meV in the activation energy. The second-order rate constant for reduction of the T1 site amounts to 2.9 × 10<sup>4</sup> M<sup>-1</sup> s<sup>-1</sup>. The mean of the distribution of forward ET rates is higher than the turnover rate from ensemble steady-state measurements and, thus, is not rate limiting.

Efficient and controlled electron transfer (ET) is essential for the proper course of metabolic processes like energy conversion and storage. Traditionally, ET rates in proteins are measured under single-turnover conditions using techniques like pulse radiolysis or flash photolysis, and the results are sometimes not in agreement with the results of steady-state kinetics measurements.<sup>1</sup> Study of enzyme kinetics at the single-molecule (SM) level allows direct access to monitor real-time events under steady-state conditions.<sup>2</sup> SM techniques and the underlying theoretical framework have evolved rapidly and greatly advanced our knowledge of enzyme mechanisms over the past decade.<sup>3</sup> The redox kinetics of flavin-containing cholesterol oxidase<sup>4</sup> and pentaerythritol tetranitrate reductase,<sup>5</sup> Cu-containing nitrite reductases,<sup>6</sup> and the conformational dynamics of dihydrofolate reductase,<sup>7</sup> for instance, have been studied profitably by SM techniques. In this Communication, we report the first SM measurements of the ET rate between the copper centers of a multicopper oxidase (MCO), i.e., small laccase (SLAC) from *Streptomyces coelicolor*.

MCOs catalyze the four-electron reduction of O<sub>2</sub> to H<sub>2</sub>O concomitant with oxidation of substrate molecules. Laccases belong to the family of MCOs which have been commercialized by industry owing to their ability to oxidize a wide variety of substrates. Their enzymatic machinery consists of a type 1 (T1)

Cu which accepts reducing equivalents from substrate molecules and transfers them across ~13 Å via a conserved HisCysHis motif to the Cu trinuclear cluster (TNC), where O<sub>2</sub> is converted to H<sub>2</sub>O.<sup>8</sup> The TNC is traditionally considered to be composed of a binuclear type 3 (T3) Cu pair and a normal type 2 (T2) Cu. A crucial step in the catalytic process is the transfer of an electron from the T1 Cu to the TNC, one at a time, four times to complete a turnover. Several reports exist in the literature focusing on measuring the ET rates anaerobically using pulse radiolysis and flash photolysis under single-turnover conditions.<sup>1b,c,9</sup> The pioneering studies of Farver, Pecht, et al., for instance, greatly advanced our understanding of how the electrons move and equilibrate between different redox centers and their consequences on the enzyme mechanism. However, close evaluation of these studies reveals that the measured ET rates are sometimes an order of magnitude or more lower than the turnover rates.<sup>1b,9a</sup> Although measurements under single-turnover conditions can provide valuable information about the enzyme mechanism, the observed intermediates are not necessarily similar to the intermediates occurring during steady-state turnover. Thus, there is a continuous demand for new methods to measure the ET rates during turnover.

Recently, a new principle was introduced: fluorescence-based detection of protein redox state(s) (FluRedox),<sup>10</sup> which allows monitoring the redox state changes of oxido-reductases during turnover at a high temporal resolution and at the SM level.<sup>6</sup> Not only does this method allow the study of hidden aspects of enzyme kinetics/dynamics (which are often masked by the rate-determining step in a bulk measurement), it also allows the study of the heterogeneity in a population of molecules. We make use of this principle to study the ET in SLAC.

SLAC is a homotrimer in which each monomer consists of two cupredoxin domains (Figure 1a), unlike the more common MCOs, which are three- or six-domain monomeric proteins.<sup>11</sup> However, it has a similar active-site morphology consisting of T1 and TNC sites and catalyzes the same reaction as other MCOs. It has been proposed that such trimeric proteins are evolutionary precursors to ascorbate oxidase, the 3-domain laccases and the 6-domain ceruloplasmin.<sup>12</sup> Recently, it was shown that SLAC may also differ from the common laccases in its mechanism of O<sub>2</sub> reduction, wherein a redox-active tyrosine residue (Y108) may have a participatory role.<sup>13</sup> SLAC has been structurally characterized<sup>11b,c,13b</sup> and, together with a recombinant expression system, provides excellent opportunities to study the ET in this enzyme in great detail.

Received: October 30, 2013

Published: January 29, 2014

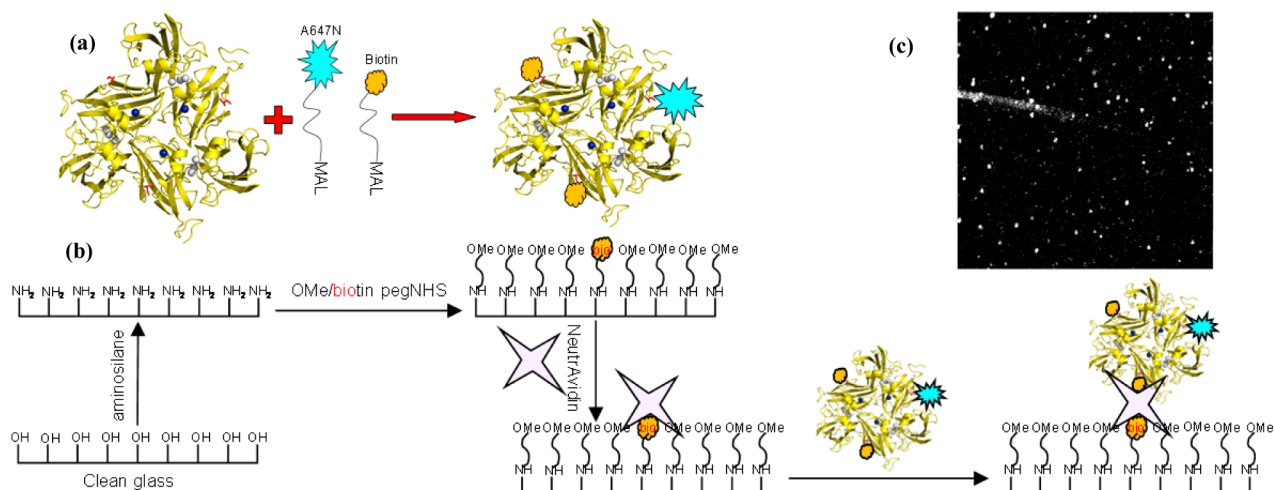


**Figure 1.** (a) K204C variant of SLAC conjugated with Atto647N-maleimide and biotin-PEG-maleimide. The conditions are chosen so that the dye-to-protein labeling ratio does not exceed 5% to ensure most enzyme molecules carry only one or no fluorescence label. T1 Cu is depicted in blue, TNC in gray, and Cys204 in red. (b) Functionalization of glass coverslips with aminosilane and PEG linkers and immobilization of SLAC conjugates using the NeutrAvidin-biotin interaction. (c) A  $40 \times 40 \mu\text{m}^2$  image taken under a confocal fluorescence microscope of the sample prepared in (b). The bright spots are individual SLAC molecules. For details about conjugation, immobilization, and confocal setup, see Supporting Information.

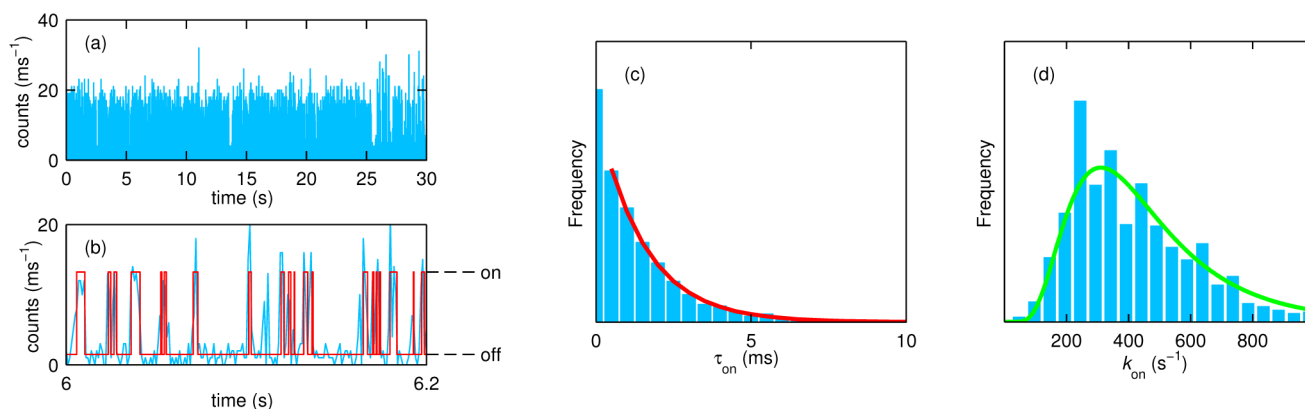


**Figure 2.** (a) Typical binned time trace (1 ms bin time) of a turning over single SLAC molecule. The molecule shows fluctuations between the high and low emission rates as the redox state of T1 Cu changes, which can be seen more clearly from a small portion of the trace as shown in (b). The red trace in (b) is bin-free and was obtained from the changepoint analysis. (c) The dwell time ( $\tau_{\text{on}}$ ) distribution of the molecule in the on-state from the trace shown in (a). The number of "on" intervals present in this trace amounted to 2767. The red line is the monoexponential fit to the normalized data with a decay constant  $k_{\text{on}} = 660 \text{ s}^{-1}$ . (d) Distribution of  $k_{\text{on}}$  obtained from  $\sim 720$  molecules of SLAC. The green line is the fit corresponding to a log-normal distribution with a mean value of  $450 \text{ s}^{-1}$ . The measurements reported in panels (a)–(c) were made in 20 mM MOPS buffer (pH 7.4) and at  $20^\circ\text{C}$  with DMPD and ascorbate concentrations of 5 and 10 mM, respectively. The data reported in panel (d) represent measurements that were performed at concentrations of DMPD varying from 0.02 to 5 mM.

To selectively label SLAC, K204C and R203C variants were prepared which contain a surface-exposed cysteine available for conjugation with thiol-reactive dyes and linkers.<sup>14</sup> When oxidized, the enzyme exhibits absorption bands at 330 and 590 nm, the latter characteristic of the T1 Cu site. The 590 nm absorption overlaps with the emission of the Atto647N dye; thus, when using SLAC labeled with this dye, the fluorescence of the dye is quenched by means of Förster resonance energy transfer (FRET) from the fluorophore to the T1 Cu chromophore. The 590 nm absorption band is absent when the enzyme is reduced, in which case the fluorescence is recovered. Thus, the emission from the enzyme–dye conjugate can serve as a highly sensitive probe of the redox state of the T1 Cu. Such fluorescence switching of the labeled variants was verified in bulk when the enzyme was cycled between oxidized and reduced states (Figure S3). Further experiments focused on the K204C variant. The enzyme was conjugated with thiol-reactive biotin-PEG linkers to

make it suitable for surface immobilization.<sup>14</sup> A cartoon depicting the labeling strategy is shown in Figure 1a.

SLAC molecules must be immobilized on a transparent solid support before any measurements can be made on a confocal microscope. A number of methods are described in the literature for immobilization of proteins on a surface.<sup>15</sup> It was an additional interest for us to immobilize SLAC in a site-specific manner. To achieve this, the glass coverslips were functionalized as shown in Figure 1b.<sup>14</sup> Briefly, clean coverslips were first functionalized with 3-(2-aminoethyl)aminopropyl trimethoxysilane to create an amine-terminated hydrophilic surface. This functionalized surface was further treated with PEG linkers containing an amine-reactive end (NHS ester) and a biotin or methoxy group at the other terminus. It was demonstrated previously that the PEG linkers minimize nonspecific adsorption of the protein on the surface.<sup>16</sup> The ratio of biotin-terminated PEG to methoxy-terminated PEG on the surface was kept below 0.1%. The SLAC

conjugates prepared earlier were then tethered to the surface via biotin-NeutrAvidin interactions (Figure 1b). This labeling and immobilization strategy helps ensure that the label/linkers attach to the protein at a specific site and minimize any heterogeneity in the sample preparation. A typical confocal image of immobilized SLAC molecules on a coverslip prepared by the above method is shown in Figure 1c.

When the laser is focused on one of the molecules, the variation in fluorescence count rate with time can be observed. In the absence of substrate, the fluorescence intensity is low and, apart from statistical noise, no fluorescence fluctuations are observed, indicating that the enzyme is in a stable oxidized state (Figure S4). In the presence of excess reductant under aerobic conditions and with the TNC selectively inhibited by incubation with cyanide, a high fluorescence intensity is observed and no fluctuations are observed, either (Figure S4), indicating that the T1 site is in a stably reduced state. The two experiments demonstrate that ET between the excited label and the T1 Cu in either the reduced or the oxidized form does not occur at a measurable rate. However, under aerobic conditions and in the presence of *N,N*-dimethyl-*p*-phenylenediamine (DMPD) as a mediator and ascorbate as a substrate, the enzyme starts to turn over, and discrete fluctuations in the emission count rates can be observed.<sup>14</sup> A typical measurement is shown in Figure 2a,b. We ascribe these fluctuations to ET from the T1 Cu to the TNC (high to low fluorescence) and from the substrate or the TNC to the T1 Cu (low to high fluorescence).

Data were collected in a photon-by-photon manner. Since only the arrival times are recorded, it is common to bin the data to visualize the count rate fluctuations. Such binning generally limits the time resolution of the experimental analysis. Thus, we made use of a bin-free method, a so-called changepoint analysis, which utilizes Bayesian statistics to analyze the raw data and to determine the time points when the molecule switches from one state to another.<sup>17</sup> It is evident from Figure 2b that the red trace obtained by such an analysis overlaps well with the binned trace. Thereafter, the dwell times in the on-state were binned, and a histogram of these dwell times was obtained (Figure 2c).<sup>14</sup> As can be seen from the fit in Figure 2c, the distribution of dwell times in the on-state follows a single-exponential decay and directly provides a rate constant ( $\sim 660 \text{ s}^{-1}$  in this example) which we equate to the rate of ET from T1 to TNC, denoted by  $k_{\text{T1} \rightarrow \text{TNC}} \equiv k_{\text{on}}$ .<sup>3b</sup> We measured time trajectories of  $\sim 720$  molecules where the DMPD concentration was varied between 0.02 and 5 mM and obtained ET rate constants in the manner discussed above. It appears that the logarithm of the rate constants can be well fitted by a Gaussian distribution (Figure S6). Thus, the rate constants follow a log-normal distribution with an arithmetic mean of  $k_{\text{T1} \rightarrow \text{TNC}} = 460 \text{ s}^{-1}$ , corresponding to a normal distribution of activation energies.<sup>18</sup> The distribution of ET rates appears quite broad and demonstrates the heterogeneity that exists from one molecule to another (*vide infra*). While in bulk experiments the catalytic reaction rate depends on substrate concentration, it is gratifying to note that the  $k_{\text{on}}$  distributions are concentration independent (Figure S7a,b), which confirms that we are dealing with an intramolecular process.

In a similar way, the off-times were analyzed. Since they appear dependent on the DMPD concentration, they could not be combined into a single data set for analysis as had been done for the on-time analysis (see above). The data sets obtained at 50  $\mu\text{M}$  and 5 mM DMPD were large enough to allow a preliminary analysis, which resulted in  $k_{\text{TNC} \rightarrow \text{T1}} = 85 \text{ s}^{-1}$  and a second-order

rate constant  $k_s = 2.9 \times 10^4 \text{ M}^{-1} \text{ s}^{-1}$ .<sup>14</sup> From the ratio of the two internal ET rate constants and associated variances, a driving force of 43 meV can be derived. The bimolecular rate constant is smaller than the rate constant measured in the bulk ( $1.3 \times 10^5 \text{ M}^{-1} \text{ s}^{-1}$ ; Figure S2). We ascribe the difference to how the enzyme is present: free in solution vs labeled and immobilized on a solid support.

A number of features are worth pointing out. First, the waiting time distributions can be fit by monoexponential decays (see Figure 2c, for example). Apparently, on the time scale of the experiment (0.5–120 s), the distribution of ET rates (Figure 2d) is static. Second, since four ET steps are needed to complete the enzyme cycle, the differences between the  $k$ 's for the different steps must be small ( $<20\%$  of the mean). This is in line with relatively small changes in driving force for the T1–TNC ET step as the TNC fills up with electrons.<sup>19</sup> Third, the internal ET rate is larger than the turnover rate measured under substrate saturating conditions in the bulk (Figure S2). This means that the frequent transitions between on- and off-states that we observe are due, in large measure, to jumps of electrons back and forth between the TNC and the T1 site. Moreover, since no long on-times—of the duration of the enzyme turnover time—were observed, a long-lived four-electron-reduced state is not part, apparently, of the enzyme cycle. It is conceivable that, after loading the TNC with two or three electrons, charge compensation is necessary through the uptake of protons and/or through dehydroxylation involving a rearrangement of the water and H-bonding network around the TNC before any further electrons can enter the T1 site. Another possibility is that a reversible conformational change temporarily switches off the T1 site, as suggested for the homologous Cu-containing nitrite reductase.<sup>20</sup> A more extensive exploration of this finding must await further experiments.

The distribution in rates may be connected with intrinsic and extrinsic causes. Enzyme immobilization on solid surfaces may lead to (partial) loss of activity. In the present study, we investigate only enzyme molecules that were still active after immobilization. The distribution of forward ET rates in Figure 2d is ascribed, thus, to intrinsic causes and is related to the thermodynamics of the catalytic process. In view of the average distance between the T1 Cu and the TNC ( $\sim 13 \text{ \AA}$ ) and the distance dependence of the electronic coupling ( $H_{\text{DA}}$ ) between the donor (T1 Cu) and the acceptor (TNC) ( $H_{\text{DA}} = k_0 \exp\{-\beta(r - r_0)\}$ ), we can calculate (with  $\beta = 1 \text{ \AA}^{-1}$ ) an activationless ( $\Delta G^0 = -\lambda$ ) ET rate constant  $k^0 = 3.7 \times 10^8 \text{ s}^{-1}$ .<sup>14</sup> Using semiclassical Marcus theory and mean and variance of the  $k_{\text{on}}$  distribution obtained from Figure 2d, an estimate of 0.347 eV for the activation energy ( $\Delta G^\ddagger$ ) can be calculated. Using a value of 43 meV for the driving force, a value for the reorganization energy  $\lambda = 1.5 \text{ eV}$  is obtained which is in line with the reorganization energy of other metalloenzymes including laccases.<sup>1a,14,21</sup> The spread in the activation energy, corresponding to the  $k_{\text{on}}$  distribution, amounts to  $\pm 28 \text{ meV}$ , which would be equivalent to a spread in the driving force of  $\pm 56 \text{ meV}$  or a spread in  $\lambda$  of  $\pm 110 \text{ meV}$ .

A similar analysis can be performed for the back ET rates. The rates obtained at  $[\text{DMPD}] = 50 \mu\text{M}$  can be used for this purpose since the contribution of the bimolecular reaction to the observed rates is negligibly small in this case.<sup>14</sup> We find an activation energy of 390 meV with a spread of  $\pm 25 \text{ meV}$ , which leads to a value for the reorganization energy of  $\lambda = 1.5 \text{ eV}$ . As expected, the spread in activation energies for the forward and backward ET is the same within the experimental uncertainty.



Gray and Winkler argued that, with the available experimental and theoretical methods, it is difficult to obtain values of  $\lambda$  to a precision that is better than  $\pm 100$  meV.<sup>21a</sup> It is surprising to realize that such a small uncertainty is compatible with the distribution in ET rates that is observed in the present SM measurements. Thus, the distribution that initially appears quite broad relates to a rather narrow distribution of  $\Delta G^\ddagger$  ( $\pm 28$  meV). A similar observation was reported earlier for copper proteins.<sup>22</sup>

In pulse radiolysis experiments on SLAC, it was reported that the ET rate increases as the TNC acquires electrons, one at a time.<sup>9b</sup> Moreover, the smallest and the largest ET rates that could be measured in those experiments amounted to  $\sim 15$  and  $186$  s<sup>-1</sup>, respectively. However, within the time resolution of the current measurements, we do not observe such a variation of ET rates, as the dwell time distribution fits to a single exponential (*vide supra*). Moreover, in the ensemble steady-state measurements at pH 6, enzymatic rates in excess of  $300$  s<sup>-1</sup> were measured, which is faster than the ET rate that could be obtained from the pulse radiolysis experiments.<sup>13b</sup> It has been shown for ascorbate oxidase that the presence of oxygen enhances the ET rate by structural perturbation of the TNC.<sup>1b,c</sup> Very recently, it was demonstrated with stopped-flow measurements on *Rhus vernicifera* laccase that the so-called native intermediate (or freshly cycled enzyme) is capable of transferring electrons (from T1 Cu to TNC) at a much higher rate than the resting enzyme.<sup>21c</sup> Although the “cycled” form of SLAC was used in the pulse radiolysis experiments, the experimental setup may not allow the experiment to proceed quickly enough so as to prevent the (partial) decay of the native intermediate to the resting form of SLAC. This might explain the difference between the previous and the current experiments. Nevertheless, the above points clearly emphasize the fact that a more reliable way to measure such a rate would be to do it during the enzyme turnover.

We are in the process of performing more experiments to analyze the correlation with the bulk measurements. The method reported here may be applicable to study ET in virtually any redox enzyme with a suitable fluorophore, provided that the enzyme exhibits distinctly different absorption spectra in the reduced and oxidized states.

## ■ ASSOCIATED CONTENT

### Supporting Information

Experimental details and off-times analysis. This material is available free of charge via the Internet at <http://pubs.acs.org>.

## ■ AUTHOR INFORMATION

### Corresponding Author

canters@chem.leidenuniv.nl

### Notes

The authors declare no competing financial interest.

## ■ ACKNOWLEDGMENTS

We thank Prof. Haw Yang for kindly providing the changepoint analysis algorithm that was used for the data analysis. We gratefully acknowledge generous support by the research programme of the Foundation for Fundamental Research on Matter (FOM), by the Chemical Sciences TOP programme, both of which are (partly) financed by the Netherlands Organisation for Scientific Research (NWO), and by the European Commission through the EdRox Network (contract no. MRTN-CT-2006-035649).

## ■ REFERENCES

- (1) (a) Farver, O.; Pecht, I. *Coord. Chem. Rev.* **2011**, *255*, 757. (b) Farver, O.; Wherland, S.; Pecht, I. *J. Biol. Chem.* **1994**, *269*, 22933. (c) Tollin, G.; Meyer, T. E.; Cusanovich, M. A.; Curir, P.; Marchesini, A. *Biochim. Biophys. Acta* **1993**, *1183*, 309.
- (2) Special Issue on Single-Molecule Spectroscopy. *Acc. Chem. Res.* **2005**, *38*, 503.
- (3) (a) English, B. P.; Min, W.; van Oijen, A. M.; Lee, K. T.; Luo, G.; Sun, H.; Cherayil, B. J.; Kou, S. C.; Xie, X. S. *Nat. Chem. Biol.* **2006**, *2*, 87. (b) Smiley, R. D.; Hammes, G. G. *Chem. Rev.* **2006**, *106*, 3080. (c) van Oijen, A. M.; Loparo, J. J. *Annu. Rev. Biophys.* **2010**, *39*, 429.
- (4) Lu, H. P.; Xun, L.; Xie, X. S. *Science* **1998**, *282*, 1877.
- (5) Pudney, C. R.; Lane, R. S.; Fielding, A. J.; Magennis, S. W.; Hay, S.; Scrutton, N. S. *J. Am. Chem. Soc.* **2013**, *135*, 3855.
- (6) (a) Kuznetsova, S.; Zauner, G.; Aartsma, T. J.; Engelkamp, H.; Hatzakis, N.; Rowan, A. E.; Nolte, R. J.; Christianen, P. C.; Canters, G. W. *Proc. Natl. Acad. Sci. U.S.A.* **2008**, *105*, 3250. (b) Goldsmith, R. H.; Tabares, L. C.; Kostrz, D.; Dennison, C.; Aartsma, T. J.; Canters, G. W.; Moerner, W. E. *Proc. Natl. Acad. Sci. U.S.A.* **2011**, *108*, 17269. (c) Tabares, L. C.; Kostrz, D.; Elmalk, A.; Andreoni, A.; Dennison, C.; Aartsma, T. J.; Canters, G. W. *Chem.—Eur. J.* **2011**, *17*, 12015.
- (7) Zhang, Z.; Rajagopalan, P. T.; Selzer, T.; Benkovic, S. J.; Hammes, G. G. *Proc. Natl. Acad. Sci. U.S.A.* **2004**, *101*, 2764.
- (8) (a) Solomon, E. I.; Sundaram, U. M.; Machonkin, T. E. *Chem. Rev.* **1996**, *96*, 2563. (b) Solomon, E. I.; Augustine, A. J.; Yoon, J. *Dalton Trans.* **2008**, 3921.
- (9) (a) Farver, O.; Wherland, S.; Koroleva, O.; Loginov, D. S.; Pecht, I. *FEBS J.* **2011**, *278*, 3463. (b) Farver, O.; Tepper, A. W.; Wherland, S.; Canters, G. W.; Pecht, I. *J. Am. Chem. Soc.* **2009**, *131*, 18226. (c) Wherland, S.; Farver, O.; Pecht, I. *ChemPhysChem* **2005**, *6*, 805.
- (10) Kuznetsova, S.; Zauner, G.; Schmauder, R.; Mayboroda, O. A.; Deelder, A. M.; Aartsma, T. J.; Canters, G. W. *Anal. Biochem.* **2006**, *350*, 52.
- (11) (a) Machczynski, M. C.; Vijgenboom, E.; Samyn, B.; Canters, G. W. *Protein Sci.* **2004**, *13*, 2388. (b) Skalova, T.; Dohnalek, J.; Ostergaard, L. H.; Ostergaard, P. R.; Kolenko, P.; Duskova, J.; Stepankova, A.; Hasek, J. *J. Mol. Biol.* **2009**, *385*, 1165. (c) Skalova, T.; Duskova, J.; Hasek, J.; Stepankova, A.; Koval, T.; Ostergaard, L. H.; Dohnalek, J. *Acta Crystallogr., Sect. F: Struct. Biol. Cryst. Commun.* **2011**, *67*, 27.
- (12) Nakamura, K.; Go, N. *Cell. Mol. Life Sci.* **2005**, *62*, 2050.
- (13) (a) Tepper, A. W. J. W.; Milikisyants, S.; Sottini, S.; Vijgenboom, E.; Groenen, E. J. J.; Canters, G. W. *J. Am. Chem. Soc.* **2009**, *131*, 11680. (b) Gupta, A.; Nederlof, I.; Sottini, S.; Tepper, A. W.; Groenen, E. J.; Thomassen, E. A.; Canters, G. W. *J. Am. Chem. Soc.* **2012**, *134*, 18213. (14) See Supporting Information.
- (15) (a) Wong, L. S.; Khan, F.; Micklefield, J. *Chem. Rev.* **2009**, *109*, 4025. (b) Heering, H.; Canters, G. W. In *Engineering the Bioelectronic Interface: Applications to Analyte Biosensing and Protein Detection*; Davis, J. J., Ed.; 2010; p 120 (c) Durán, N.; Rosa, M. A.; D'Annibale, A.; Gianfreda, L. *Enzyme Microb. Technol.* **2002**, *31*, 907.
- (16) (a) Prime, K. L.; Whitesides, G. M. *Science* **1991**, *252*, 1164. (b) Ha, T.; Rasnik, I.; Cheng, W.; Babcock, H. P.; Gauss, G. H.; Lohman, T. M.; Chu, S. *Nature* **2002**, *419*, 638. (c) Rasnik, I.; Myong, S.; Cheng, W.; Lohman, T. M.; Ha, T. *J. Mol. Biol.* **2004**, *336*, 395.
- (17) Watkins, L. P.; Yang, H. *J. Phys. Chem. B* **2005**, *109*, 617.
- (18) McKinney, S. A.; Joo, C.; Ha, T. *Biophys. J.* **2006**, *91*, 1941.
- (19) Tepper, A. W. J. W.; Aartsma, T. J.; Canters, G. W. *Faraday Discuss.* **2011**, *148*, 161.
- (20) Strange, R. W.; Murphy, L. M.; Dodd, F. E.; Abraham, Z. H.; Eady, R. R.; Smith, B. E.; Hasnain, S. S. *J. Mol. Biol.* **1999**, *287*, 1001.
- (21) (a) Gray, H. B.; Winkler, J. R. *Q. Rev. Biophys.* **2003**, *36*, 341. (b) Voityuk, A. A. *J. Phys. Chem. B* **2011**, *115*, 12202. (c) Heppner, D. E.; Kjaergaard, C. H.; Solomon, E. I. *J. Am. Chem. Soc.* **2013**, *135*, 12212.
- (22) (a) Salverda, J. M.; Patil, A. V.; Mizzon, G.; Kuznetsova, S.; Zauner, G.; Akkiliç, N.; Canters, G. W.; Davis, J. J.; Heering, H. A.; Aartsma, T. J. *Angew. Chem., Int. Ed.* **2010**, *49*, 5776. (b) Davis, J. J.; Burgess, H.; Zauner, G.; Kuznetsova, S.; Salverda, J.; Aartsma, T.; Canters, G. W. *J. Phys. Chem. B* **2006**, *110*, 20649.